Journal of Magnetic Resonance **142,** 199–204 (2000)
Article ID jmre.1999.1976, available online at http://www.idealibrary.com on IDEAL®

Sensitivity Enhancement in Solid State ^{15}N NMR by Indirect Detection with High-Speed Magic Angle Spinning

Yoshitaka Ishii and Robert Tycko

Laboratory of Chemical Physics, National Institute of Diabetes and Digestive and Kidney Diseases, National Institutes of Health, Bethesda, Maryland 20892

E-mail: tycko@helix.nih.gov

Received October 26, 1999

Enhancement of sensitivity in solid state ^{15}N NMR by indirect detection through ^{1}H NMR signals under high-speed magic angle spinning and high-field conditions is demonstrated experimentally on two ^{15}N-labeled peptides, polycrystalline AlaGlyGly and the helix-forming, 17-residue peptide MB(i + 4)EK in lyophilized form. Sensitivity enhancement factors ranging from 2.0 to 3.2 are observed experimentally, depending on the ^{15}N and ^{1}H linewidths and polarization transfer efficiencies. The ^{1}H-detected two-dimensional ^{1}H/^{15}N correlation spectrum of AlaGlyGly illustrates the possibility of increased spectral resolution and resonance assignments in indirectly detected experiments, in addition to the sensitivity enhancement.

Key Words: **solid state NMR; magic angle spinning; indirect detection; nitrogen-15 NMR; peptides.**

Sensitivity enhancement by indirect detection in heteronuclear double-resonance NMR measurements has been extensively employed in solid state NMR by high-field (*1–5*) and field-cycling (*6, 7*) techniques, as well as in high-resolution liquid state NMR (*8–12*). Indirect detection of ^{15}N and ^{13}C spectra via ^{1}H NMR signals now forms the basis of modern multidimensional spectroscopic techniques for resonance assignment and structure determination of biopolymers in liquid state NMR. The large sensitivity enhancements in liquid state NMR result from the efficiency and specificity of heteronuclear polarization transfer techniques that are based on scalar couplings, and from the narrowness of ^{1}H NMR lines in liquids. In contrast, measurements of ^{15}N and ^{13}C spectra in solid state NMR of organic and biomolecular systems, as well as spectra of other nuclei with low magnetogyric ratios, are conventionally carried out with direct detection. This is because the ^{1}H NMR lines in solids are usually so broad that there is no sensitivity advantage to indirect detection. However, recent technological developments, in particular the commercial availability of magic angle spinning (MAS) probes capable of stable spinning frequencies in excess of 30 kHz and the availability of homogeneous magnets with fields of 17.6 T and higher, led us to reexamine the possibility of sensitivity enhancement by indirect detection in solid state NMR. In this Communication, we show that significant sensitivity enhancements are indeed possible in ^{15}N NMR spectroscopy of polypeptides in solid form at high fields and with high-speed MAS.

In this section, we derive the frequency-domain signal-to-noise (S/N) ratios (per root time) for a signal from spin-$\frac{1}{2}$ nucleus X in directly detected one-dimensional (1D) and indirectly detected two-dimensional (2D) NMR measurements. The S/N of the directly detected experiment may be derived in accordance with the treatment of Ernst *et al.* (*13*) as

$$(\mathrm{S/N})_{DD} = \frac{\langle s_\mathrm{X}(t) w_\mathrm{X}(t)\rangle}{\langle w_\mathrm{X}(t)^2\rangle^{1/2}} (R t^{\max})^{1/2} \frac{A_\mathrm{X}}{\rho_\mathrm{X}}, \qquad [1]$$

where $w_\mathrm{X}(t)$ is an apodization window function, $t^{\max}$ is the length of the acquired time domain signal, and $\langle z\rangle$ denotes the time average of z over the interval $[0, t^{\max}]$. R is the repetition rate for signal averaging. The normalized 1D time-domain NMR signal of X is assumed to be of the form $A_\mathrm{X} s_\mathrm{X}(t)\exp(-i\omega_\mathrm{X} t)$, where $s_\mathrm{X}(t)$ is a nonnegative envelope function with $s_\mathrm{X}(0) = 1$, and ω_X is the resonant frequency for the X nuclei. ρ_X is the square root of the noise power spectral density per unit frequency. Following Abragam (*14*), $A_\mathrm{X}/\rho_\mathrm{X}$ can be expressed as

$$\frac{A_\mathrm{X}}{\rho_\mathrm{X}} = \left(\frac{\pi\omega_\mathrm{X} V Q_\mathrm{X}}{kT}\right)^{1/2} \eta M_\mathrm{X}, \qquad [2]$$

where M_X is the initial X spin magnetization (i.e., magnetic moment per volume), T is temperature, and V, η, and Q_X are the volume, filling factor, and quality factor of the sample coil for X detection. Assuming that M_X is created by cross polarization from ^{1}H spins with polarization transfer efficiency f, we find $M_\mathrm{X} = f\gamma_\mathrm{H}\gamma_\mathrm{X}\hbar^2 B_0 N_\mathrm{X}/4kT$, where N_X is the number density of X nuclei, γ_H and γ_X are the magnetogyric ratios of the

1090-7807/00

X and ^{1}H nuclei, and B_0 is the applied magnetic field. Equation [1] then becomes

$$(\mathrm{S/N})_{DD} = f(\gamma_X B_0)^{3/2}\gamma_H \frac{\langle s_X(t) w_X(t)\rangle}{\langle w_X(t)^2\rangle^{1/2}} (t^{\max})^{1/2} Q_X^{1/2} C_X, \quad [3]$$

where C_X is a constant that subsumes properties such as temperature, coil geometry, filling factor, receiver noise figure, spin density, and repetition rate for signal averaging.

The frequency-domain signal-to-noise ratio in a 2D indirect detection measurement, in which the ^{1}H NMR signals detected in t_2 are modulated at the X NMR frequencies in t_1, may be derived similarly from the expression (*13*)

$$(\mathrm{S/N})_{ID} = \frac{\langle s(t_1, t_2) w(t_1, t_2)\rangle}{2^{1/2}\langle w(t_1, t_2)^2\rangle^{1/2}} (R t_2^{\max})^{1/2} \frac{A_H}{\rho_H}, \quad [4]$$

where $s(t_1, t_2)$ is the normalized envelope function of the 2D time-domain signal with $s(0, 0) = 1$, $w(t_1, t_2)$ is a window function for the 2D data, $t_k^{\max}(k = 1, 2)$ is the maximum t_k value, and $\langle z(t_1, t_2)\rangle$ denotes the time average of z over the intervals $[0, t_1^{\max}]$ and $[0, t_2^{\max}]$. A_H is the ^{1}H NMR signal amplitude at $t_1 = t_2 = 0$ and ρ_H is the square root of the noise power spectral density per unit frequency for ^{1}H detection. In analogy to Eq. [2],

$$\frac{A_H}{\rho_H} = \left(\frac{\pi\omega_H V Q_H}{kT}\right)^{1/2} \eta M_H, \quad [5]$$

where M_H denotes the ^{1}H magnetization at $t_1 = t_2 = 0$, ω_H is the ^{1}H NMR frequency, and Q_H is the quality factor of the sample coil for ^{1}H detection. Additionally assuming that spin polarization is transferred from X nuclei to ^{1}H nuclei between the t_1 and t_2 periods with efficiency $(N_X/N_H) f$, where N_H is the number density of ^{1}H nuclei that contribute to the detected ^{1}H NMR line ($N_H \geq N_X$), we find $M_H = f^2\gamma_H^2\hbar^2 B_0 N_X/4kT$. Equation [4] becomes

$$(\mathrm{S/N})_{ID} = 2^{-1/2} f^2 (\gamma_H B_0)^{3/2}\gamma_H \times \frac{\langle s(t_1, t_2) w(t_1, t_2)\rangle}{\langle w(t_1, t_2)^2\rangle^{1/2}} (t_2^{\max})^{1/2} Q_H^{1/2} C_H, \quad [6]$$

where C_H is a constant analogous to C_X. If direct and indirect detection experiments are performed at the same temperature using a probe with a single double-tuned sample coil for X and ^{1}H nuclei, we can assume $C_H \approx C_X$.

When the 2D signal can be separated as $s(t_1, t_2) = s_X(t_1)s_H(t_2)$ and $w(t_1, t_2) = w_X(t_1)w_H(t_2)$, Eq. [2] can be rewritten as

$$(\mathrm{S/N})_{ID} = \frac{f^2}{\sqrt{2}} (\gamma_H B_0)^{3/2}\gamma_H \times \frac{\langle s_X w_X\rangle\langle s_H w_H\rangle}{\langle w_X^2\rangle^{1/2}\langle w_H^2\rangle^{1/2}} (t_2^{\max})^{1/2} Q_H^{1/2} C_H. \quad [7]$$

Assuming $C_X = C_H$ and $t^{\max} = t_1^{\max}$, the sensitivity enhancement factor ξ for indirect detection becomes

$$\xi \equiv \frac{(\mathrm{S/N})_{ID}}{(\mathrm{S/N})_{DD}} = \frac{f}{\sqrt{2}} \left(\frac{\gamma_H}{\gamma_X}\right)^{3/2} \frac{\langle s_H w_H\rangle}{\langle w_H^2\rangle^{1/2}} \left(\frac{t_2^{\max}}{t_1^{\max}}\right)^{1/2} \left(\frac{Q_H}{Q_X}\right)^{1/2}. \quad [8]$$

ξ is optimized when a matched filter is used for w_H, i.e., $s_H(t) = w_H(t)$. Then, Eq. [8] becomes

$$\xi = \frac{f}{\sqrt{2}} \left(\frac{\gamma_H}{\gamma_X}\right)^{3/2} \left(\frac{\langle s_H^2\rangle t_2^{\max}}{t_1^{\max}}\right)^{1/2} \left(\frac{Q_H}{Q_X}\right)^{1/2} = \frac{f}{\sqrt{2\kappa}} \left(\frac{\gamma_H}{\gamma_X}\right)^{3/2} \left(\frac{W_X}{W_H}\right)^{1/2} \left(\frac{Q_H}{Q_X}\right)^{1/2} \quad [9]$$

with

$$\kappa \equiv 2\pi t_1^{\max} W_X \quad [10]$$

$$W_X \equiv (2\pi t_1^{\max}\langle s_X^2\rangle)^{-1} \quad [11a]$$

$$W_H \equiv (2\pi t_2^{\max}\langle s_H^2\rangle)^{-1}. \quad [11b]$$

The expressions in Eqs. [11] represent general definitions of the NMR linewidths (units of Hz) in the X and ^{1}H spectra. These expressions reduce to the conventional full-width-at-half-maximum (FWHM) for Lorentzian lineshapes and to the FWHM times $(2\pi \ln 2)^{-1/2} \approx 0.479$ for Gaussian lineshapes in the limit of large $t_k^{\max}$. When a matched filter is applied to maximize the sensitivity, $t_1^{\max}$ and $t^{\max}$ are typically selected to be $\sim 1/(2W_X)$, which yields $\kappa \sim \pi$. In static or slow MAS experiments on a rigid organic solid, W_H is typically 40 kHz. If $f = 0.5$, $\kappa = \pi$, $Q_H/Q_X = 2$, and $W_X = 100$ Hz, which may be typical values, then $\xi = 0.112$ for X = ^{13}C and $\xi = 0.437$ for X = ^{15}N. There is no gain in sensitivity. However, if $W_H = 500$ Hz, then $\xi = 1.00$ for X = ^{13}C and $\xi = 3.91$ for X = ^{15}N. Thus, substantial sensitivity gains are possible for nuclei with low γ if the ^{1}H NMR lines can be made narrow and polarization transfer can be made efficient.

Experiments were carried out on a Bruker DMX-750 spectrometer, using a Bruker double-resonance MAS probe with rotor diameters of 2.5 mm. This probe has a double-tuned, single coil design with $Q_X \approx 76$ and $Q_H \approx 220$. Figure 1 shows ^{1}H MAS NMR spectra of a 9 mg sample of polycrystalline L-alanylglycylglycine (AlaGlyGly), acquired at 17.6 T (749.6

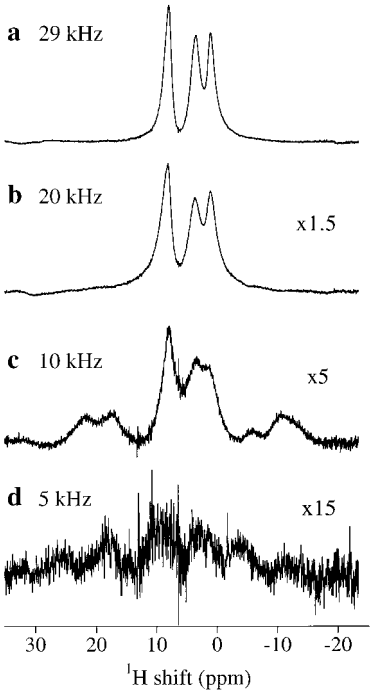

FIG. 1. Dependence of the ^{1}H MAS NMR spectrum of AlaGlyGly powder (9 mg) on spinning frequency, observed at 749.6 MHz (17.6 T field). Signal was excited by a 7.5 μs $\pi/2$ pulse. Spinning speeds are indicated. The vertical scale of the figure is expanded by a factor of 1.5, 5, and 15 in (b), (c), and (d), respectively.

MHz ^{1}H NMR frequency) with spinning frequencies ν_R ranging from 5 to 29 kHz. In this sample, 15% of the AlaGlyGly molecules are ^{15}N-labeled at the amino nitrogen of Ala1 and the amide nitrogens of Gly2 and Gly3. The labeled molecules are diluted in unlabeled AlaGlyGly by recrystallization. High-speed MAS produces a dramatic enhancement in resolution and sensitivity, as previously shown by other groups (*15–22*). At $\nu_R = 29$ kHz, three lines with widths of 1.2 to 1.5 ppm are resolved, arising from the amino and amide protons (8.2 ppm), the alpha protons (3.8 ppm), and the methyl protons (1.1 ppm).

Figure 2 shows a radiofrequency (RF) pulse sequence for ^{1}H-detected two-dimensional (2D) ^{1}H/^{15}N correlation spectroscopy. Polarization transfer from ^{1}H to ^{15}N is accomplished with adiabatic cross-polarization (*23*), using a tangential pulse shape at the ^{15}N frequency. During the t_1 period, a weak proton decoupling field (10 kHz amplitude), which gives the best resolution in the ^{15}N NMR spectrum at large ν_R, is applied. A pair of $\pi/2$ pulses are applied to ^{15}N spins at the end of the t_1 period to spin-lock either the real or imaginary component of the ^{15}N polarization for transfer back to ^{1}H spins. ^{1}H free-induction decay signals are acquired during t_2 without heteronuclear decoupling. The tangential pulse shape for ^{15}N spins is given by $\omega_{1X}(t) = \omega_1^0 \pm \omega_\Delta \tan[\alpha(t - \tau/2)]/[2 \tan(\alpha\tau/2)]$, where ω_1^0 is the average RF amplitude, ω_Δ is width of modulation of the RF amplitude, α is the rate of modulation, and τ is the pulse length, where $0 \leq t \leq \tau$.

Figure 3a shows the ^{15}N NMR spectrum of the triply ^{15}N-labeled AlaGlyGly sample at $\nu_R = 29$ kHz, as obtained with direct ^{15}N detection (76.0 MHz NMR frequency) following adiabatic cross-polarization using the tangential pulse described above. The lines at 38.9, 104.5, and 108.6 ppm arise from the nitrogens of Ala1, Gly2, and Gly3, respectively. Figure 3b shows the ^{1}H-detected ^{15}N NMR spectrum of the same sample, with the same total number of scans, the same spinning frequency, and the same NMR probe and spectrometer, extracted as a single slice from the full 2D ^{1}H/^{15}N correlation spectrum shown in Fig. 3c. Under the conditions of these measurements, the ^{15}N NMR linewidths are 1.0 ppm and the ^{1}H NMR linewidths are as shown in Fig. 1. Lorentzian line broadening of 1.0 ppm is applied in Fig. 3a. The maximum t_1 value for Figs. 3b and 3c is 6.4 ms. Gaussian line broadening of 1.2 ppm in t_2 and Lorentzian line broadening of 1.0 ppm in t_1 are applied in Figs. 3b and 3c. The signal-to-noise ratio in the indirectly detected ^{15}N spectrum (Fig. 3b) is higher than that in the directly detected spectrum (Fig. 3a) by a factor of $\xi = 2.0$.

In addition to sensitivity enhancements, 2D indirect detection experiments can provide information that is potentially useful for assignments and structural studies. For instance, Fig. 3c shows a weak crosspeak between methyl ^{1}H (1 ppm) and amino ^{15}N (39 ppm), reflecting the proximity of the amino ^{15}N and methyl ^{1}H. This crosspeak confirms the assignment of the ^{15}N resonance at 39 ppm to Ala1 of AlaGlyGly. Indirect detection could be used as an aid to resonance assignments in larger peptides and proteins that are ^{15}N-labeled at multiple sites. A longer cross polarization period or an additional ^{1}H–^{1}H mixing period may permit us to obtain longer-range distance information. Moreover, ^{1}H chemical shifts are available in indirect detection experiments, possibly providing useful information on the hydrogen bonding state of NH groups. In Fig. 3c, ^{1}H chemical shifts of NH groups (8.25 ppm) are resolved from that of the NH_3 group (8.0 ppm), while these chemical shifts are not resolved in the 1D spectra in Fig. 1.

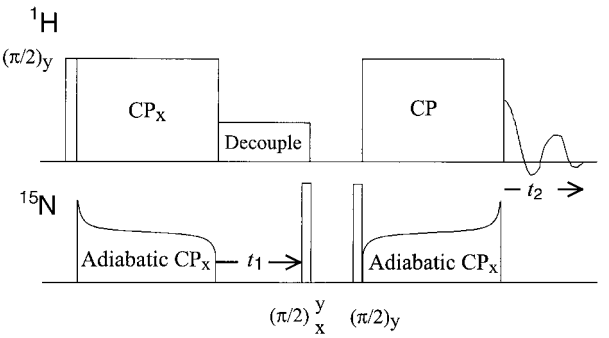

FIG. 2. Pulse sequence for ^{1}H-detected 2D ^{1}H/^{15}N correlation spectroscopy. Magnetization of ^{15}N spins is prepared with adiabatic cross polarization using a tangential shaped pulse at the ^{15}N frequency. During the t_1 period, a ^{1}H decoupling field is applied. After the t_1 period, a pair of $\pi/2$ pulses are applied to select the real or imaginary component of the ^{15}N magnetization, which is transferred back to ^{1}H spins with the reversed tangential pulse.

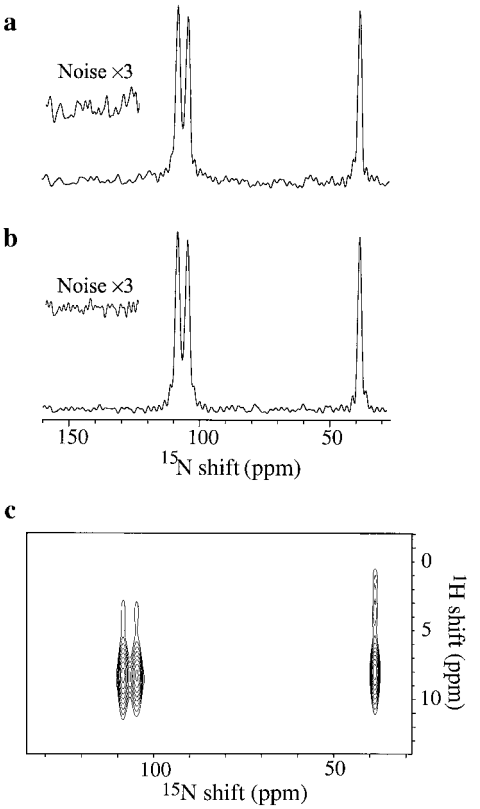

FIG. 3. ^{15}N MAS NMR spectra of a 9 mg polycrystalline sample of triply-^{15}N-labeled AlaGlyGly (15% labeled molecules diluted in 85% unlabeled molecules), with 28.9 kHz spinning frequency. (a) Directly detected spectrum. ^{15}N magnetization was prepared using adiabatic cross polarization with a tangential shape pulse, with parameters $\omega_1^0/2\pi = 20$ kHz, $\omega_\Delta/2\pi = 16$ kHz, $\alpha = 750$ rad/s, and $\tau = 4$ ms. ^{1}H RF field amplitude was 49 kHz during cross polarization and 10 kHz during ^{15}N signal acquisition. Matched filter was applied with 1.0 ppm Lorentzian broadening to maximize the sensitivity. (b) Indirectly detected spectrum, obtained with the pulse sequence in Fig. 2. ^{1}H decoupling amplitude in t_1 was 10 kHz. Gaussian line broadening of 1.2 ppm in t_2 and Lorentzian line broadening of 1.0 ppm in t_1 were applied. This spectrum is a one-dimensional slice at 7.4 ppm from the 2D ^{1}H/^{15}N correlation spectrum shown in (c). A total of 256 scans were acquired for each of the spectra in (a) and (b), and $t_1^{max} = t^{max} = 6.4$ ms.

The enhancement factor ξ increases with increasing ^{15}N linewidths. The ^{15}N linewidths in polycrystalline AlaGlyGly are narrower than those in typical noncrystalline samples, which show inhomogeneous broadening due to structural disorder. Therefore, additional experiments were performed on a 5 mg lyophilized sample of the synthetic helical peptide MB(i + 4)EK (*24–26*) (amino acid sequence Ac–AE-AAAKEAAAKEAAAKA–NH_2, where Ac represents an acetyl group), with ^{15}N labels at the amide nitrogens of Ala9 and Ala10. Figure 4a shows the directly detected ^{15}N NMR spectrum of this sample, obtained at $\nu_R = 28.3$ kHz. The two ^{15}N labels give rise to a single line at 118 ppm with a width of 4.9 ppm. No line broadening is applied in Fig. 4a to show the maximum resolution. Figure 4b shows the ^{1}H-detected ^{15}N spectrum of the same sample, obtained as a single slice from a 2D ^{1}H/^{15}N correlation spectrum, again with the same total number of scans, the same spinning frequency, and the same NMR probe and spectrometer. ^{15}N/^{1}H cross peaks for the ^{15}N–^{1}H pairs in Ala9 and Ala10 are not resolved in the 2D ^{15}N/^{1}H correlation spectrum. The ^{15}N NMR linewidth is 4.9 ppm and the ^{1}H NMR linewidth for amide protons is 1.2 ppm. The maximum t_1 value for Fig. 4b is 2.7 ms. Gaussian line broadening of 1.2 ppm is applied in t_2. No line broadening is applied in t_1. The signal-to-noise ratio in the indirectly detected spectrum (Fig. 4b) is higher than that in the directly detected spectrum (Fig. 4a) by a factor of $\xi = 3.2$.

The experimental results for AlaGlyGly and MB(i + 4)EK demonstrate that significant enhancements in sensitivity are possible for ^{15}N MAS NMR with indirect detection at high spinning speeds. The observed values of ξ (2.0 and 3.2) are significantly greater than one, but are somewhat less than the theoretical values (3.6 and 5.5) calculated under the assumptions leading to Eq. [9], with $f = 0.4$ and the Q_H, Q_X, t_1^{max}, and Gaussian ^{1}H linewidths stated above. The value of f is estimated by comparing ^{15}N signal intensities obtained with adiabatic cross polarization and fast MAS to those obtained with standard cross polarization (i.e., with unmodulated RF amplitudes) and slow MAS, and assuming $f = 0.5$ in the latter case. The differences between experimental and theoretical enhancement factors may arise in part from uncertainties in f and from the fact that some ^{15}N polarization is lost through polarization transfer from ^{15}N to ^{1}H nuclei that are not directly bonded, i.e., that contribute to ^{1}H NMR lines other than the amino/amide line.

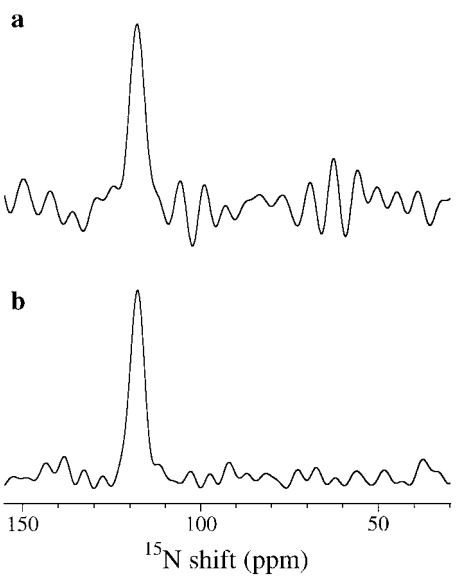

FIG. 4. ^{15}N MAS NMR spectra of a 5 mg sample of doubly-^{15}N-labeled MB(i + 4)EK obtained with direct detection (a) and indirect detection (b). Experimental conditions were the same as in Fig. 3, except that 512 scans were acquired for each spectrum, spinning frequency was 28.3 kHz and $t_1^{max} = t^{max} = 2.7$ ms. Matched filter was applied only to ^{1}H dimension in the indirectly detected spectrum. The indirectly detected spectrum is a single slice at 7.9 ppm from a 2D ^{1}H/^{15}N correlation spectrum, as in Fig. 3c.

With ^{1}H NMR linewidths of approximately 1.0 kHz, indirect detection of ^{13}C MAS NMR spectra is unlikely to afford a sensitivity advantage. Further increases in ξ may be possible through more efficient polarization transfer. Ideal adiabatic polarization transfer yields $f = 1.0$ for an isolated ^{13}C–^{1}H pair. Higher MAS frequencies may produce narrower ^{1}H lines and make indirect detection advantageous. ξ is expected to increase with increasing B_0 in many cases, both because spin diffusion among protons is suppressed by chemical shift differences and because W_X/W_H will increase when W_X is determined by inhomogeneous broadening and W_H is determined by residual proton–proton couplings. Even if indirect detection does not increase sensitivity, ^{13}C/^{1}H correlations available from indirectly detected spectra may provide useful structural or assignment information. Sensitivity enhancements for other, lower-γ nuclei may be even larger than those observed for ^{15}N. Among spin-$\frac{1}{2}$ nuclei, ^{57}Fe, ^{89}Y, ^{103}Rh, ^{107}Ag, ^{109}Ag, ^{169}Tm, ^{183}W, and ^{187}Os may be interesting candidates for indirect detection.

With indirect detection, the sensitivity of ^{15}N solid state NMR of biopolymers becomes comparable to the sensitivity of ^{13}C solid state NMR. Because available quantities of isotopically labeled biochemical samples are usually severely limited, ^{13}C-based structural measurements have usually been preferred. Indirect detection promises to make ^{15}N-based measurements, such as measurements of ^{15}N–^{15}N distances or ^{15}N–^{15}N correlations with dipolar recoupling techniques (*27–38*), feasible in many biochemical systems. Measurements of heteronuclear interactions (*39*), such as ^{15}N–^{13}C and ^{15}N–^{1}H dipole–dipole couplings, or heteronuclear correlations (*21, 40, 41*) may also benefit from indirect detection.

ACKNOWLEDGMENTS

This work was supported in part by the NIH Intramural AIDS Targeted Antiviral Program. Y.I. received postdoctoral fellowship support from the Japan Society for the Promotion of Science.

REFERENCES

1. N. Bloembergen and P. P. Sorokin, Nuclear magnetic resonance in the cesium halides, *Phys. Rev.* **110,** 865–875 (1958).
2. S. R. Hartmann and E. L. Hahn, Nuclear double resonance in the rotating frame, *Phys. Rev.* **128,** 2042–2053 (1962).
3. F. M. Lurie and C. P. Slichter, Spin temperature in nuclear double resonance, *Phys. Rev. A* **133,** 1108–1122 (1964).
4. P. Mansfield and P. K. Grannell, Improved resolution of small resonance shifts of dilute nuclear spin systems in solids by pulsed double resonance, *J. Phys. C* **4,** L197–L200 (1971).
5. A. Pines, M. G. Gibby, and J. S. Waugh, Proton-enhanced NMR of dilute spins in solids, *J. Chem. Phys.* **59,** 569–590 (1973).
6. A. G. Redfield, Pure nuclear electric quadrupole resonance in impure copper, *Phys. Rev.* **130,** 589–595 (1963).
7. R. E. Slusher and E. L. Hahn, Sensitive detection of nuclear quadrupole interactions in solids, *Phys. Rev.* **166,** 332–347 (1968).
8. A. A. Maudsley, L. Müller, and R. R. Ernst, Cross-correlation of spin-decoupled NMR spectra by heteronuclear two-dimensional spectroscopy, *J. Magn. Reson.* **28,** 463–469 (1977).
9. L. Müller, Sensitivity enhanced detection of weak nuclei using heteronuclear multiple quantum coherence, *J. Am. Chem. Soc.* **101,** 4481–4484 (1979).
10. A. Bax, R. H. Griffey, and B. L. Hawkins, Correlation of proton and nitrogen-15 chemical shifts by multiple quantum NMR, *J. Magn. Reson.* **55,** 301–315 (1983).
11. G. Bodenhausen and D. J. Ruben, Natural abundance nitrogen-15 NMR by enhanced heteronuclear spectroscopy, *Chem. Phys. Lett.* **69,** 185–189 (1980).
12. A. G. Redfield, Stimulated echo NMR spectra and their use for heteronuclear two-dimensional shift correlation, *Chem. Phys. Lett.* **96,** 537 (1983).
13. R. R. Ernst, G. Bodenhausen, and A. Wokaun, "Principles of Nuclear Magnetic Resonance in One and Two Dimensions," pp. 148–153, 349–354, Oxford University Press, Oxford, 1987.
14. A. Abragam, "Principles of Nuclear Magnetism," pp. 82–83, Oxford Univ. Press, New York, 1961.
15. K. Zilm, A. Mehta, B. Tounge, S. Burns, G. Coker, J. Gehman, and A. Luptak, High resolution solids NMR of uniformly labeled macromolecular building blocks: the potential of high field solids NMR in chemical biology, *in* "39th Experimental Nuclear Magnetic Resonance Conference," Asilomar, 1998.
16. C. Filip, S. Hafner, I. Schnell, D. E. Demco, and H. W. Spiess, Solid-state nuclear magnetic resonance spectra of dipolar-coupled multi-spin systems under fast magic angle spinning, *J. Chem. Phys.* **110,** 423–440 (1999).
17. R. Graf, D. E. Demco, S. Hafner, and H. W. Spiess, Selective residual dipolar couplings in cross-linked elastomers by H-1 double-quantum NMR spectroscopy, *Solid State Nucl. Magn. Reson.* **12,** 139–152 (1998).
18. I. Schnell, A. Lupulescu, S. Hafner, D. E. Demco, and H. W. Spiess, Resolution enhancement in multiple-quantum MAS NMR spectroscopy, *J. Magn. Reson.* **133,** 61–69 (1998).
19. S. Hafner and H. W. Spiess, Multiple-pulse assisted line-narrowing by fast magic-angle spinning, *Solid State Nucl. Magn. Reson.* **8,** 17–24 (1997).
20. S. Hafner and H. W. Spiess, Multiple-pulse line narrowing under fast magic-angle spinning, *J. Magn. Reson. Ser. A* **121,** 160–166 (1996).
21. B. J. vanRossum, G. J. Boender, and H. J. M. deGroot, High magnetic field for enhanced proton resolution in high-speed CP/MAS heteronuclear H-1-C-13 dipolar-correlation spectroscopy, *J. Magn. Reson. Ser. A* **120,** 274–277 (1996).
22. S. Ray, E. Vinogradov, G. J. Boender, and S. Vega, Proton MAS NMR spectra at high magnetic fields and high spinning frequencies: Spectral simulations using Floquet theory, *J. Magn. Reson.* **135,** 418–426 (1998).
23. S. Hediger, B. H. Meier, and R. R. Ernst, Adiabatic passage Hartmann-Hahn cross polarization in NMR under magic angle sample spinning, *Chem. Phys. Lett.* **240,** 449–456 (1995).
24. H. W. Long and R. Tycko, Biopolymer conformational distributions from solid-state NMR: alpha-helix and 3(10)-helix contents of a helical peptide, *J. Am. Chem. Soc.* **120,** 7039–7048 (1998).
25. S. Marqusee, V. H. Robbins, and R. L. Baldwin, Unusually Stable Helix Formation in Short Alanine-Based Peptides, *Proc. Natl. Acad. Sci. U.S.A.* **86,** 5286–5290 (1989).
26. S. Marqusee and R. L. Baldwin, Helix Stabilization By Glu− . . . Lys+ Salt Bridges in Short Peptides of Denovo Design, *Proc. Natl. Acad. Sci. U.S.A.* **84,** 8898–8902 (1987).
27. R. Tycko and G. Dabbagh, Measurement of nuclear magnetic

dipole-dipole couplings in magic angle spinning NMR, *Chem. Phys. Lett.* **173,** 461–465 (1990).

28. R. Tycko and S. O. Smith, Symmetry Principles in the Design of Pulse Sequences For Structural Measurements in Magic Angle Spinning Nuclear-Magnetic-Resonance, *J. Chem. Phys.* **98,** 932–943 (1993).

29. A. E. Bennett, D. P. Weliky, and R. Tycko, Quantitative conformational measurements in solid state NMR by constant-time homonuclear dipolar recoupling, *J. Am. Chem. Soc.* **120,** 4897–4898 (1998).

30. D. M. Gregory, D. J. Mitchell, J. A. Stringer, S. Kiihne, J. C. Shiels, J. Callahan, M. A. Mehta, and G. P. Drobny, Windowless dipolar recoupling—the detection of weak dipolar couplings between spin-$\frac{1}{2}$ nuclei with large chemical-shift anisotropies, *Chem. Phys. Lett.* **246,** 654–663 (1995).

31. A. E. Bennett, C. M. Rienstra, J. M. Griffiths, W. G. Zhen, P. T. Lansbury, and R. G. Griffin, Homonuclear radio frequency-driven recoupling in rotating solids, *J. Chem. Phys.* **108,** 9463–9479 (1998).

32. A. E. Bennett, J. H. Ok, R. G. Griffin, and S. Vega, Chemical shift correlation spectroscopy in rotating solids: radio frequency-driven dipolar recoupling and longitudinal exchange, *J. Chem. Phys.* **96,** 8624–8627 (1992).

33. M. Hohwy, C. M. Rienstra, C. P. Jaroniec, and R. G. Griffin, Fivefold symmetric homonuclear dipolar recoupling in rotating solids: Application to double quantum spectroscopy, *J. Chem. Phys.* **110,** 7983–7992 (1999).

34. B. Q. Sun, P. R. Costa, D. Kocisko, P. T. Lansbury, and R. G. Griffin, Internuclear distance measurements in solid-state nuclear-magnetic-resonance–dipolar recoupling via rotor Synchronized spin locking, *J. Chem. Phys.* **102,** 702–707 (1995).

35. D. P. Raleigh, M. H. Levitt, and R. G. Griffin, Rotational resonance in solid state NMR, *Chem. Phys. Lett.* **146,** 71–76 (1988).

36. Y. K. Lee, N. D. Kurur, M. Helmle, O. G. Johannessen, N. C. Nielsen, and M. H. Levitt, Efficient Dipolar Recoupling in the Nmr of Rotating Solids—a Sevenfold Symmetrical Radiofrequency Pulse Sequence, *Chem. Phys. Lett.* **242,** 304–309 (1995).

37. Y. Ishii and T. Terao, Manipulation of nuclear spin Hamiltonians by rf-field modulations and its applications to observation of powder patterns under magic-angle spinning, *J. Chem. Phys.* **109,** 1366–1374 (1998).

38. M. Baldus, M. Tomaselli, B. H. Meier, and R. R. Ernst, Broad-band polarization-transfer experiments for rotating solids, *Chem. Phys. Lett.* **230,** 329–336 (1994).

39. T. Gullion, Measurement of Heteronuclear Dipolar Interactions by Rotational-Echo, Double-Resonance Nuclear Magnetic Resonance, *Magn. Reson. Rev.* **17,** 83–131 (1997).

40. B. J. vanRossum, H. Forster, and H. J. M. deGroot, High-field and high-speed CP-MAS C-13 NMR heteronuclear dipolar-correlation spectroscopy of solids with frequency-switched Lee-Goldburg homonuclear decoupling, *J. Magn. Reson.* **124,** 516–519 (1997).

41. A. Lesage, D. Sakellariou, S. Steuernagel, and L. Emsley, Carbon-proton chemical shift correlation in solid-state NMR by through-bond multiple-quantum spectroscopy, *J. Am. Chem. Soc.* **120,** 13194–13201 (1998).